Journal of Hazardous Materials 217–218 (2012) 43–50

Contents lists available at SciVerse ScienceDirect

Journal of Hazardous Materials

journal homepage: www.elsevier.com/locate/jhazmat

Enhancing the adsorption of vapor-phase mercury chloride with an innovative composite sulfur-impregnated activated carbon

Iau-Ren Ie[a], Wei-Chin Chen[a], Chung-Shin Yuan[a,*], Chung-Hsuang Hung[b], Yuan-Chung Lin[a], Hsieh-Hung Tsai[a], Yi-Shiu Jen[a]

[a] Institute of Environmental Engineering, National Sun Yat-Sen University, No. 70, Lian-Hai Road, Kaohsiung 804, Taiwan, ROC
[b] Department of Safety, Health and Environmental Engineering, National Kaohsiung First University of Science and Technology No. 2, Juoyue Road, Nantz District, Kaohsiung 811, Taiwan, ROC

ARTICLE INFO

Article history:
Received 24 August 2011
Received in revised form 13 February 2012
Accepted 13 February 2012
Available online 21 February 2012

Keywords:
Thermogravimetric analysis (TGA)
Vapor-phase mercury chloride ($HgCl_2$)
Composite sulfurized activated carbons
Surface characteristics and chemical properties
Adsorptive capacity

ABSTRACT

Mercury chloride ($HgCl_2$) is the major mercury derivate emitted from municipal solid waste incinerators, which has high risk to the environment and human health. This study investigated the adsorption of vapor-phase $HgCl_2$ with an innovative composite sulfurized activated carbon (AC), which was derived from the pyrolysis, activation, and sulfurization of waste tires. The composite sulfur-impregnation process impregnated activated carbon with aqueous-phase sodium sulfide (Na_2S) and followed with vapor-phase elemental sulfur (S^0). Thermogravimetric analysis (TGA) was applied to investigate the adsorptive capacity of vapor-phase $HgCl_2$ using the composite sulfurized AC. The operating parameters included the types of composite sulfurized AC, the adsorption temperature, and the influent $HgCl_2$ concentration. Experimental results indicated that the sulfur-impregnation process could increase the sulfur content of the sulfurized AC, but decreased its specific surface area. This study further revealed that the composite sulfurized AC impregnated with aqueous-phase Na_2S and followed with vapor-phase S^0 ($Na_2S + S^0$ AC) had much higher saturated adsorptive capacity of $HgCl_2$ than AC impregnated in the reverse sequence ($S^0 + Na_2S$ AC). A maximum saturated adsorptive capacity of $HgCl_2$ up to 5236 μg-$HgCl_2$/g-C was observed for the composite $Na_2S + S^0$ AC, which was approximately 2.00 and 3.17 times higher than those for the single Na_2S and S^0 ACs, respectively.

1. Introduction

Since 1991, twenty-two regional municipal solid waste (MSW) incinerators have been built in Taiwan to deal with MSW and overcome the problem of limited space available for landfills in urban areas. However, MSW is often mixed with many kinds of harmful substances, and generally these cannot be completely removed through incineration, even when air pollution control devices (APCDs) are used [1]. Among the harmful substances produced, heavy metals are most difficult to deal with, and mercury containing compounds are particularly hazardous air pollutants (HAPs) that present the highest risk to the environment and human health. Mercury and its derivatives (e.g. mercury chloride and mercury oxide) have a very high vapor pressure, and they are highly volatile in the high temperature environment of MSW incinerators, and can be easily emitted into the atmosphere. Consequently, if they cannot be effectively eliminated by APCDs, then they can cause severe secondary pollution problems.

The production of activated carbons derived from the pyrolysis of waste tires is considered a feasible technology [2–6], and it is now possible to generate approximately 32–42% by mass of carbon blacks associated with pyrolyzed oil and combustible gasses [7,8]. Carbon blacks can be further derived to produce activated carbons in the activation temperature range of 800–900 °C, and applied to adsorb volatile organic compounds (VOCs) and heavy metals, such as mercury.

The adsorption of elemental mercury (Hg^0) and mercury chloride ($HgCl_2$) by sulfur impregnated activated carbons (ACs) has been conducted with thermogravimetric analysis (TGA) technology [9,10]. These studies investigated the adsorptive capacity of Hg^0 or $HgCl_2$ under various adsorption conditions (e.g. adsorption temperature and the influent concentration of Hg^0 or $HgCl_2$). TGA is often used to investigate the changes in the weight of the tested substances under constant or variable temperature conditions, and to obtain the pyrolysis rate of waste tires and the adsorption rate of VOCs adsorbed onto granular activated carbon [11,12]. Moreover, TGA has also been applied to determine the

* Corresponding author. Tel.: +886 7 5252000x4409; fax: +886 7 52524409.
E-mail address: ycsngi@mail.nsysu.edu.tw (C.-S. Yuan).

0304-3894/$ – see front matter © 2012 Elsevier B.V. All rights reserved.
doi:10.1016/j.jhazmat.2012.02.035

adsorptive capacity of $HgCl_2$ [8]. The change of AC's weight was considered as the adsorbed $HgCl_2$ on the surface of AC. Previous studies showed that the adsorption of $HgCl_2$ decreases with adsorption temperature. However, when other chemical additives (e.g. sulfur and sodium sulfide) are impregnated to AC, the $HgCl_2$ adsorptive capacity of the impregnated AC can be enhanced [8,13,14]. Activated carbons with high surface areas generally have high adsorptive capacity, indicating that active sites for sulfur bonding are formed during the formation of the pore structure [15]. The sulfur content of AC generally increases with adsorption temperature due to a shift of the adsorption mechanism from physical adsorption to chemisorption [16]. The gas temperature in the TGA reaction chamber can be programmally controlled. An AC sample was loaded on a crucible holder (6 mm i.d. × 3 mm) inside the TGA reaction chamber and nitrogen gas (protective gas) entered the TGA reaction chamber at a flow rate of 10 mL/min before the adsorption experiments were conducted. The reactive gas that contained $HgCl_2$ entered the TGA reaction chamber and contacted with AC until the saturation adsorption of AC was reached. Graydon et al. investigated the impregnation of AC with gas-phase SO_2, and found that it enhanced the removal efficiency of elemental mercury (Hg^0) in relatively high temperature environments [17]. The surface characteristics of AC can be changed and the adsorptive capacity of a specific pollutant increases when other chemical substances are added to AC. For instance, the saturated adsorptive capacity of $HgCl_2$ increases remarkably after sulfur impregnation. Therefore, it might be worthwhile to combine different sulfur additives (e.g. Na_2S and S^0) together to produce the composite sulfurized AC ($Na_2S + S^0$ AC) and hoped that the saturated adsorptive capacity of the composite sulfurized AC ($Na_2S + S^0$ AC) could be higher than each single sulfurized AC (Na_2S AC or S^0 AC).

Activated carbons have been widely used for the removal of organic compounds (e.g. dioxins) and heavy metals (e.g. $HgCl_2$) in the flue gases emitted from MSW incinerators. However, as the temperature of flue gases is mostly higher than 150 °C in the MSW incinerators, these results in lower adsorption efficiency of $HgCl_2$. Impregnating AC with additives could overcome this problem [18]. Applying TGA to the adsorption of heavy metals by AC is rare, although it has been widely used to study the adsorption of VOCs. While studies have been conducted on impregnating AC with S^0 or Na_2S separately to remove vapor-phase $HgCl_2$ [19–21], none have been conducted to investigate the adsorption of vapor-phase $HgCl_2$ with a composite sulfur-impregnated AC ($S^0 + Na_2S$). Therefore, this study aims to enhance the adsorptive capacity of vapor-phase $HgCl_2$ by using an innovative composite sulfur-impregnated AC.

2. Experimental methods

In this work, carbon black derived from waste tires was tested herein. A tubular oven made of stainless steel was designed to activate carbon black to activated carbon. Approximately 2.5 g of carbon black was placed in a ceramic crucible at the center of the tubular oven in the absence of oxygen. The activation of carbon black was performed at 900 °C and 1 atm. In this study, H-AC, M-AC, and L-AC with the specific surface area of 766, 476, and 250 m^2/g was generated at an activation temperature of 900 °C for 180, 120, and 60 min, respectively, by using a water feed rate of 1.0 $mgH_2O/gC\text{-}s$. Prior to the $HgCl_2$ adsorption experiments, the raw ACs were heated in an oven at 105 °C for 24 h to remove moisture and then stored in a desiccator [8]. The raw ACs were further impregnated by aqueous-phase $Na_2S(s)$ and/or gas-phase $S^0(g)$. For the preparation of Na_2S AC, $Na_2S(s)$ was dissolved in deionized water (D.I. H_2O) to prepare 3% (w/w) aqueous solution of $Na_2S(aq)$. The raw AC of approximately 1 g was impregnated in a 100 mL $Na_2S(aq)$ solution, and then dried in an oven at 105 °C for 24 h [15]. For the preparation of S^0 AC, a mixture of 0.5 g raw AC and 1.5 g $S^0(s)$ was heated at 400 °C in an oven for 3 h. The raw AC was thus impregnated with the vaporized $S^0(g)$ in the oven [21]. This study further combined two above impregnation processes to prepare the composite $Na_2S + S^0$ AC with aqueous-phase $Na_2S(aq)$ and followed with vapor-phase $S^0(g)$.

This study aims to produce an innovative composite sulfur-impregnated AC under different impregnation conditions, such as various sulfur species and impregnation temperatures, and to investigate the changes of its pore size distribution and specific surface area before and after impregnation. Furthermore, the composite sulfur-impregnation AC production procedure is verified in the sequence of aqueous-phase Na_2S followed by vapor-phase S^0 or in the reverse sequence to obtain the optimum sulfurized AC. The adsorption mechanism of vapor-phase $HgCl_2$ produced under different experimental conditions (such as adsorption temperature and influent $HgCl_2$ concentration) was examined with a TGA (Model TGA/SDTA 851e) manufactured by Mettler Toledoto. In addition, to better understand the adsorption mechanism of $HgCl_2$ for the composite sulfur-impregnated AC, this study further compares its adsorption of $HgCl_2$ with that of the single sulfur-impregnated AC.

The gas temperature in the TGA reaction chamber can be programmally controlled. The raw or sulfurized AC sample was loaded on a crucible holder (6 mm i.d. × 3 mm) placed inside the TGA reaction chamber, and nitrogen gas (protective gas) entered the TGA reaction chamber at a flow rate of 10 mL/min prior to the $HgCl_2$ adsorption experiments were conducted. The reactive gas that contained $HgCl_2$ then entered the TGA reaction chamber and contacted with AC until the equilibrium weight of AC was reached. The gain of AC's weight was considered as the adsorbed $HgCl_2$ on the surface of AC.

The experiments were divided into two phases in this study. In the first phase, the characterization of the composite sulfur-impregnated AC was undertaken, and Scanning Electron Microscopy (JEOL JSM, Model 6700F) and Environmental Scanning Electron Microscopy (FEI Quanta, Model 200) were applied to measure the surface characteristics and chemical properties of AC before and after sulfur-impregnation. In the second phase, the experiments were carried out to examine the adsorption of $HgCl_2$ by the composite sulfur-impregnated AC in a temperature programmed bench-scale experimental system, as shown in Fig. 1. An influent gas stream with a mercury chloride concentration of 100–500 $\mu g/m^3$ was generated using a dynamic calibrator (VICI Metronics, Model 450). Various concentrations of $HgCl_2$ can be obtained by adjusting the gas flow rate and the heating temperature of a permeation tube. Nitrogen gas with flow rates of 0.4–1.3 mL/min passed through the permeation tube heated to 150 °C in the dynamic calibrator to ensure the constant $HgCl_2$ concentration of 100–500 $\mu g/m^3$. During the $HgCl_2$ adsorption experiments, the changes in the mass of the composite sulfur-impregnated AC were continuously recorded with the TGA, and the dynamic adsorption curve can be drawn based on the changes in the adsorption time and the mass of AC, and consequently the adsorption rate of $HgCl_2$ can be determined [22]. The operating parameters investigated in this study included the adsorption temperature (80, 100, 150, 200, and 300 °C) and the influent $HgCl_2$ concentration (100, 300, and 500 $\mu g/m^3$). Nitrogen gas was fed into the system with the gas flow rate of 10 mL/min at the heating rate of 10–20 °C/min. In this study, the adsorptive capacities of $HgCl_2$ on H-AC, M-AC and L-AC were determined as the increased mass of H-AC, M-AC and L-AC measured with the thermogravimetric analyzer (TGA) divided by the initial mass of H-AC, M-AC and L-AC, respectively.

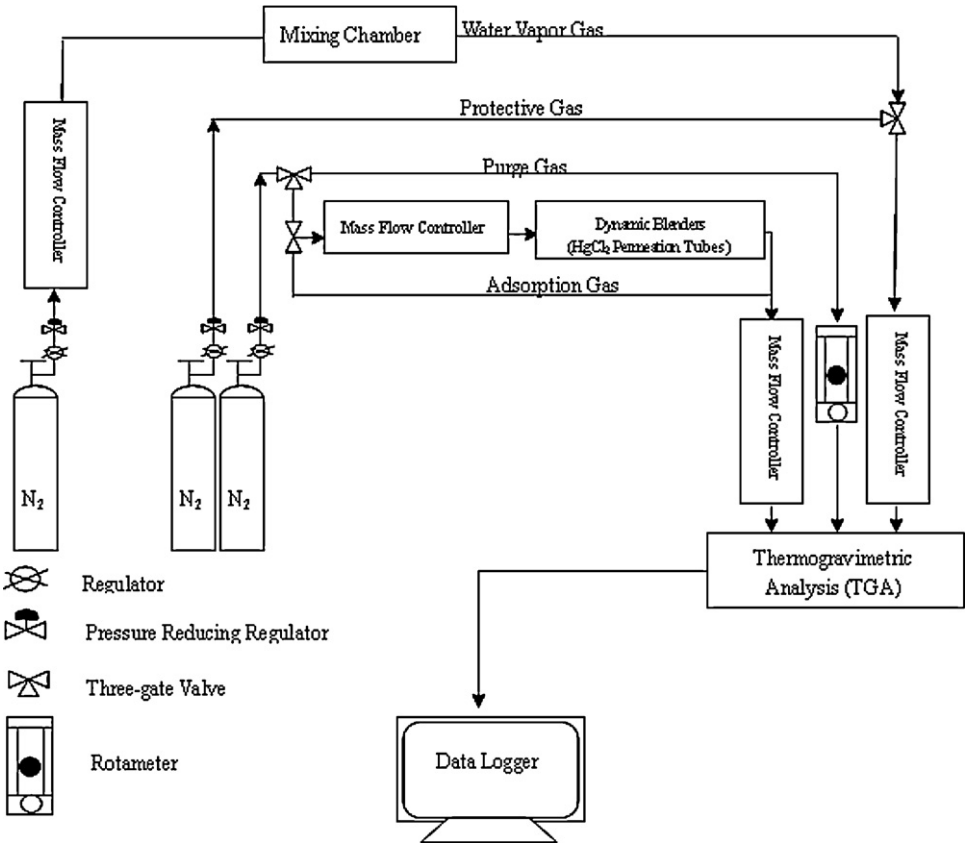

Fig. 1. Schematic diagram of the temperature programmed bench-scale experimental system for the adsorption of mercury chloride.

3. Results and discussion

3.1. Surface characteristics and chemical properties of composite sulfur-impregnated activated carbons

Prior to conducting the $HgCl_2$ adsorption experiments, the surface characteristics (i.e. specific surface area and pore volume) and chemical properties (i.e. sulfur content) of activated carbons before and after sulfur impregnation were investigated.

Pyrolysis of waste tires was used to produce carbon black which was then activated to form AC with different specific surface areas, including high- (766 m^2/g), medium- (476 m^2/g), and low-surface-area (250 m^2/g). The optimum operating parameters for producing AC with different specific surface areas have been investigated in the previous study [5,6]. Activated carbons with different surface areas were further impregnated by vapor-phase S^0 and/or aqueous-phase Na_2S to produce the composite sulfurized AC. The surface characteristics and chemical properties of AC before and after sulfur impregnation were further investigated, and are discussed in a later section.

The specific surface area (SSA) and pore volume of high-SSA ACs (H-AC), median-SSA ACs (M-AC), and low-SSA ACs (L-AC) before and after sulfur impregnation were measured with a BET surface analyzer. Table 1 summarizes micropore SSA (S_{micro}), mesopore and macropore SSA ($S_{meso+macro}$), SSA (S_{BET}), S_{micro}/S_{BET}, micropore volume (V_{micro}), total pore volume (V_{total}), and V_{micro}/V_{total} of H-AC, M-AC, and L-AC before and after sulfur impregnation. The results indicated that the SSA of the composite sulfurized H-AC, M-AC, and L-AC decreased from 766 to 196 m^2/g, from 476 to 86 m^2/g, and from 250 to 53 m^2/g, receptively, after sulfur impregnation. In other words, the SSA of all types of ACs declined after sulfur impregnation with aqueous-phase sodium sulfide (Na_2S) and vapor-phase elemental sulfur (S^0). The S_{micro}/S_{BET} and V_{micro}/V_{total} of the raw and sulfurized ACs ranged from 30.00% to 42.40% and from 6.50% to 11.11%, respectively. Both of them decreased after sulfur impregnation. The more sulfur was impregnated, the lower SSA and pore volume of sulfur-impregnated ACs were obtained. These results indicated that part of the micropores, mesopores, and macropores were probably plugged by Na_2S. Particularly, 77%, 83%, and 79% of micropore's surface areas of H-AC, M-AC, and L-AC, respectively, were reduced after sulfur impregnation.

Table 1
The specific surface area and pore volume of H-AC, M-AC, and L-AC before and after sulfur impregnation with aqueous-phase Na_2S and vapor-phase S^0.

Types of ACs	S_{micro} (m^2/g)	$S_{meso+macro}$ (m^2/g)	S_{BET} (m^2/g)	S_{micro}/S_{BET} (%)	V_{micro} (cm^3/g)	V_{total} (cm^3/g)	V_{micro}/V_{total} (%)
H-AC	253	513	766	33.03	0.083	0.918	11.11
Na_2S+S^0 H-AC	57	139	196	30.00	0.025	0.300	8.33
M-AC	150	326	476	31.51	0.066	0.686	9.62
Na_2S+S^0 M-AC	26	60	86	30.23	0.012	0.238	5.04
L-AC	106	144	250	42.40	0.048	0.436	11.01
Na_2S+S^0 L-AC	22	31	53	41.51	0.010	0.155	6.50

H-AC: high-SSA ACs; Na_2S+S^0 H-AC: Na_2S+S^0 sulfurized H-AC; M-AC: median-SSA ACs; Na_2S+S^0 M-AC: Na_2S+S^0 sulfurized M-AC; L-AC: low SSA ACs; and Na_2S+S^0 L-AC: Na_2S+S^0 sulfurized L-AC.

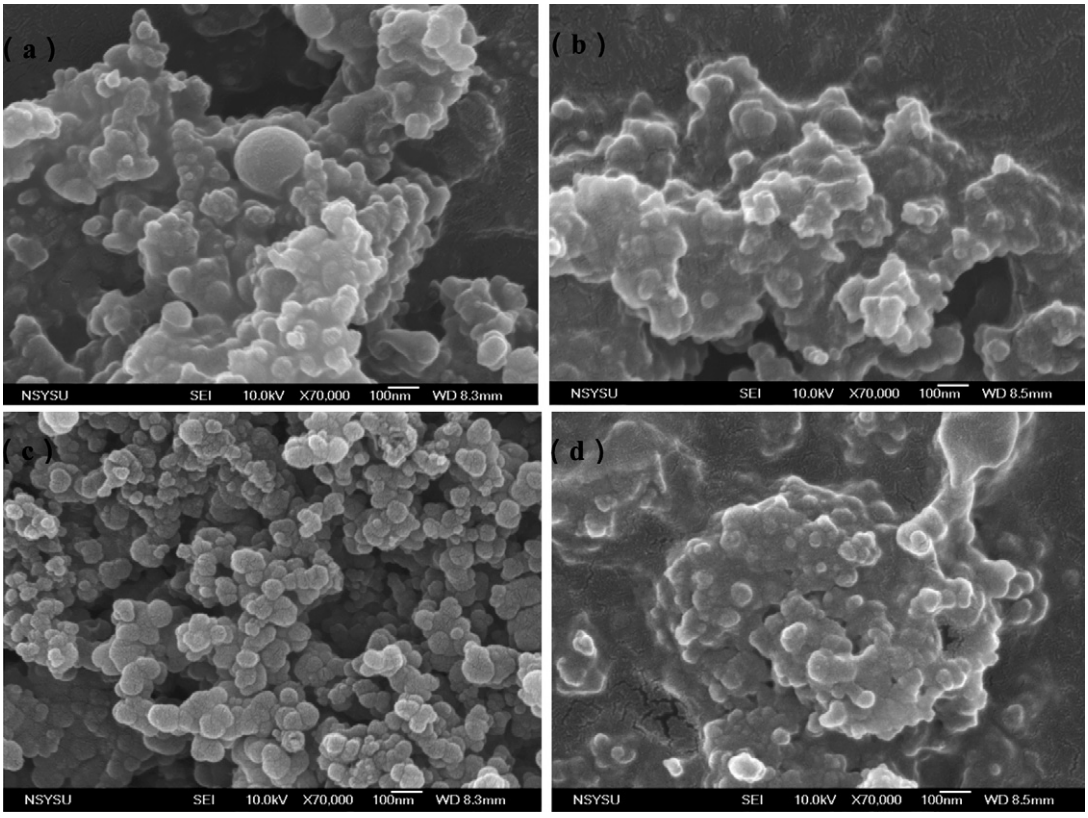

Fig. 2. The pore size and structure of H-AC before and after sulfur impregnation for (a) the raw AC, (b) the AC impregnated with vapor-phase S^0 (S^0 AC), (c) the AC impregnated with aqueous-phase Na_2S (Na_2S AC), (d) the composite sulfurized AC impregnated with aqueous-phase Na_2S and followed by vapor-phase S^0 ($Na_2S + S^0$ AC).

Microscope image showed that activated carbons contained many irregular-shaped micropores, and some of them were curved. To prove that the micropores of AC have an irregular shapes, a Transmission Electron Microscope (TEM) was used to examine them, with their surface characteristics were measured with a Scanning Electron Microscope (SEM). Fig. 2 illustrates the pore size and structure of the virgin AC, the aqueous-phase Na_2S impregnated AC, the vapor-phase S^0 impregnated AC, and the composite sulfur-impregnated AC. Most pores were macropores, with a diameter greater than 500 Å, while the transitional pores and micropores were developed and hidden inside the macropores, indicating that the AC was mostly composed of porous materials, and the layers of the pores tended to extend downward. Fig. 3 shows that the sulfur content of the virgin and sulfurized AC before and after sulfur impregnation measured with an Energy Dispersive Spectrometer (EDS). Experimental results showed that the composite sulfur-impregnation process could greatly enhance the sulfur content of AC. The sulfur content of the composite sulfur-impregnation AC (Na_2S and S^0) was mostly the sum of the sulfur content of two separate sulfur-impregnated AC (Na_2S or S^0). Furthermore, the higher the sulfur content of AC, the lower the surface area. Overall, an increase in the AC's sulfur content can effectively enhance the adsorption of $HgCl_2$. However, as the transitional pores and macropores became the main channels for adsorbates entering the micropores, the amount of transitional pores and macropores could influence the overall adsorptive capacity of AC [23,24]. Therefore, the sulfur content and specific surface area of the composite sulfur-impregnated AC were two important factors that influenced the adsorptive capacity of $HgCl_2$.

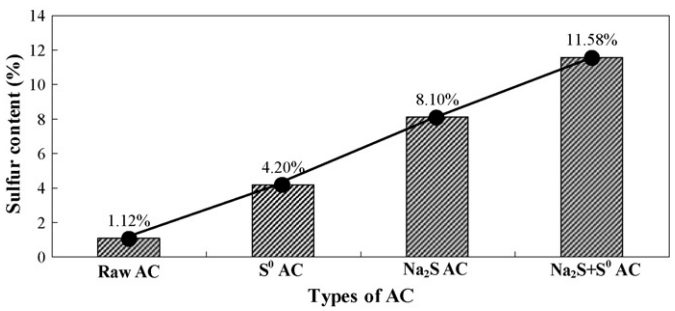

Fig. 3. The sulfur content of the raw and sulfurized AC.

3.2. Adsorption of $HgCl_2$ with composite sulfurized activated carbons

3.2.1. Adsorption of $HgCl_2$ with influent $HgCl_2$ concentration

Table 2 summarizes the corresponding adsorptive capacities of $HgCl_2$ with regard to the influent $HgCl_2$ concentrations of 100, 300, and 500 $\mu g/m^3$ for the sulfur-impregnated H-AC, M-AC, and L-AC, respectively. The adsorptive capacity of $HgCl_2$ increased, given a specific surface area, as the influent $HgCl_2$ concentration increased. Fig. 4 illustrates that, under the condition of the same specific surface area, the activated carbon's adsorptive capacity of $HgCl_2$ increased with the influent $HgCl_2$ concentration and the sulfur content of AC. The increase of $HgCl_2$ adsorption with influent $HgCl_2$ concentration is mainly attributed to the increase of mass transfer driving force resulting from the difference between the initial and equilibrium $HgCl_2$ concentrations. For the same SSA, activated carbon's saturated adsorptive capacity of $HgCl_2$ increased with the influent $HgCl_2$ concentration. It is mainly due to the increase of driving force, including the concentration gradient between influent and equilibrium $HgCl_2$ concentration and the duration required for equilibrium adsorption. Based on the theory of isotherms, the amount of adsorbates adsorbed (i.e. saturated

Table 2
Specific surface area and sulfur content of different sulfurized carbons and their adsorptive capacity of mercury chloride with specific surface area (adsorption temperature: 150 °C; nitrogen flow: 10 mL/min).

Types of ACs	Specific surface area (m^2/g)	Sulfur content (%)	Influent $HgCl_2$ concentration ($\mu g/m^3$)	Adsorptive capacity (μg-$HgCl_2$/g-C)
Na_2S+S^0 H-AC	196	11.58	500	5,236
		11.58	300	4,967
		11.58	100	4,366
Na_2S+S^0 M-AC	86	5.91	500	3,112
		5.91	300	1,919
		5.91	100	946
Na_2S+S^0 L-AC	53	5.23	500	2,222
		5.23	300	1,536
		5.23	100	941

Na_2S+S^0 H-AC: Na_2S+S^0 sulfurized H-AC; Na_2S+S^0 M-AC: Na_2S+S^0 sulfurized M-AC; and Na_2S+S^0 L-AC: Na_2S+S^0 sulfurized L-AC.

adsorptive capacity) is equilibrated with the vapor-phase concentration of adsorbates. The equilibrium gas concentration depends on the adsorbate loading for all of the adsorbents tested, and, therefore, the phenomenon under consideration is an adsorption process rather than a gas–solid reaction [15]. The comparison between the results relative to the raw AC and those relative to the impregnated AC indicated that Na_2S+S^0 AC did not change the nature of the gas–solid interaction although it increased the saturated adsorptive capacity of $HgCl_2$.

3.2.2. Adsorption of $HgCl_2$ with specific surface area of composite sulfurized activated carbons

Table 3 summarizes the corresponding adsorptive capacities of $HgCl_2$ with regard to the specific surface areas of sulfur-impregnated H-AC, M-AC, and L-AC, respectively. The adsorptive capacity of $HgCl_2$ increased with the specific surface area of the sulfur-impregnated AC for a given influent $HgCl_2$ concentration. Fig. 5 illustrates that, under the condition of the same influent $HgCl_2$ concentration, the activated carbon's adsorptive capacity of $HgCl_2$ increased with the sulfur content of activated carbons. The results showed that the specific surface areas of the composite sulfur-impregnated AC could affect the adsorptive capacity of $HgCl_2$. Figs. 4 and 5 illustrate the change of AC's weight with adsorption time, and the saturated adsorptive capacities of different ACs were obtained. A two-stage adsorption phenomenon was observed for median- and low-SSA AC (Fig. 4(b) and (c)). Particularly for low-SSA AC, relatively high percentage of S_{micro} to S_{BET} (S_{micro}/S_{BET}) resulted in the adsorption of $HgCl_2$ at macropores in the beginning and followed by the adsorption of $HgCl_2$ at micropores. For the adsorption of $HgCl_2$, although the composite sulfurized AC (Na_2S+S^0 AC) reduced the interfacial area, it definitely enhanced the saturated adsorptive capacity of AC (Figs. 4 and 5), probably due to the formation of relatively strong bonds between sulfur and mercury and/or the increase in the number of active sites for $HgCl_2$ adsorption [6,15,21]. Previous study also reported that the sulfurized ACs can more effectively remove $HgCl_2$ than the raw ACs at 150 °C [8]. Although high sulfur content reduces the specific surface area of ACs, the saturated adsorptive capacity of $HgCl_2$ is enhanced. At high temperatures, the chemical bonding force is far higher than the van der Waal's force. The sulfur bond reduces when the distance between the adsorbent and the adsorbates increases. It suggests that monolayer adsorption occurs on the surface of activated carbon due to chemisorption [15]. The reaction of $HgCl_2$ and S on the surface of ACs can be described by the following reaction [25].

$$HgCl_{2(g)} + S_{(ad)} \Rightarrow HgS_{(s)} + Cl_{2(g)}$$

3.3. Variation of $HgCl_2$ adsorptive capacity with adsorption temperature

To understand the influence of composite sulfur-impregnation on the adsorptive capacity of $HgCl_2$ under different adsorption temperatures, experiments on the adsorption of $HgCl_2$ were conducted by using composite sulfur-impregnated AC with a high specific surface area at the influent $HgCl_2$ concentration of 500 $\mu g/m^3$ and the adsorption temperatures of 80, 100, 150, 200, and 300 °C. As illustrated in Fig. 6, the corresponding adsorptive capacities of $HgCl_2$ at the adsorption temperatures of 80, 100, 150, 200, and 300 °C were 1,091, 3530, 5236, 5420 and 5848 μg-$HgCl_2$/g-C, respectively. Morimoto et al. found that the chemisorption of $HgCl_2$ for the composite sulfur-impregnated AC was enhanced at the adsorption temperatures of 80–150 °C [19]. Therefore, the adsorption of $HgCl_2$ at adsorption temperatures below 70 °C is dominated by physical adsorption, while the adsorption of $HgCl_2$ at the adsorption temperatures above 70 °C is dominated by to chemisorption. However, the AC used in this study was impregnated by vapor-phase S^0 and/or aqueous-phase Na_2S, which was different from the single sulfur-impregnation mentioned in the earlier works [26,27]. Further investigation was conducted to ascertain the initial temperature for chemisorption of $HgCl_2$ for the composite sulfur-impregnated

Table 3
Specific surface area and sulfur content of different sulfurized carbons and their adsorptive capacity of mercury chloride with influent mercury chloride concentration (adsorption temperature: 150 °C; nitrogen flow: 10 mL/min).

Influent $HgCl_2$ concentration ($\mu g/m^3$)	Types of ACs	Specific surface area (m^2/g)	Sulfur content (%)	Adsorptive capacity (μg-$HgCl_2$/g-C)
500	Na_2S+S^0 H-AC	196	11.58	5,236
	Na_2S+S^0 M-AC	86	5.91	3,112
	Na_2S+S^0 L-AC	53	5.23	2,222
300	Na_2S+S^0 H-AC	196	11.58	4,967
	Na_2S+S^0 M-AC	86	5.91	1,919
	Na_2S+S^0 L-AC	53	5.23	1,536
100	Na_2S+S^0 H-AC	196	11.58	4,366
	Na_2S+S^0 M-AC	86	5.91	946
	Na_2S+S^0 L-AC	53	5.23	941

Na_2S+S^0 H-AC: Na_2S+S^0 sulfurized H-AC; Na_2S+S^0 M-AC: Na_2S+S^0 sulfurized M-AC; and Na_2S+S^0 L-AC: Na_2S+S^0 sulfurized L-AC.

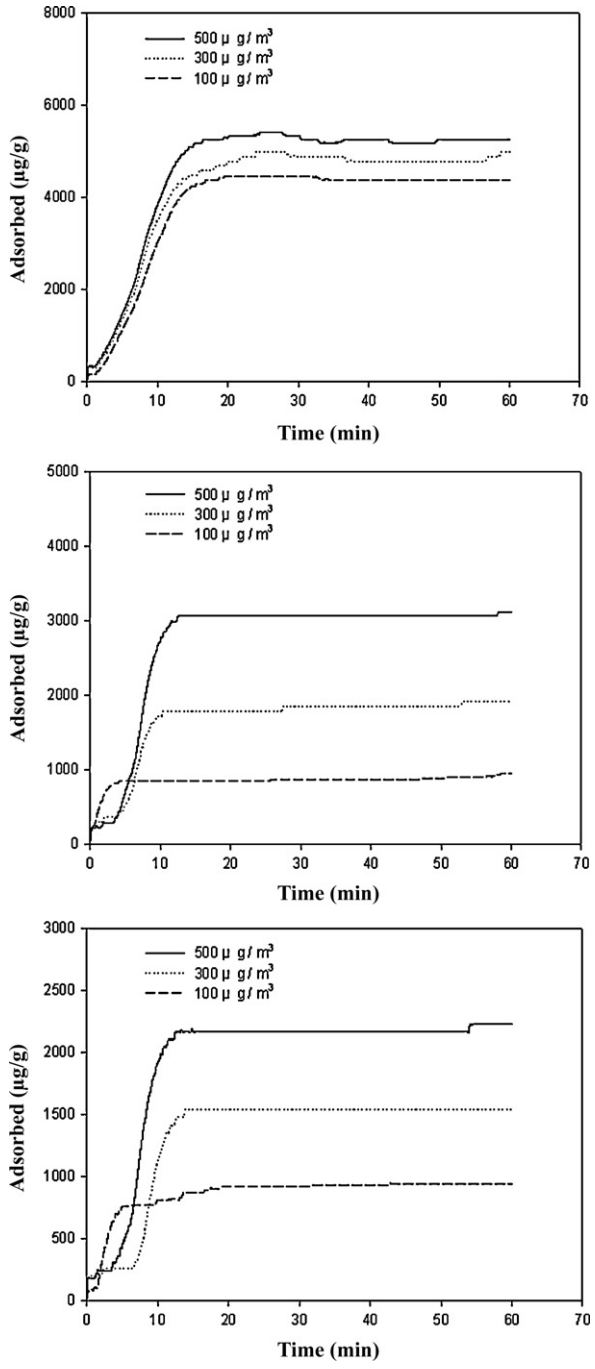

Fig. 4. The adsorption of $HgCl_2$ for different influent $HgCl_2$ concentration using Na_2S+S^0 sulfur-impregnated AC with (a) high, (b) medium, and (c) low specific surface areas (adsorption temperature: 150 °C).

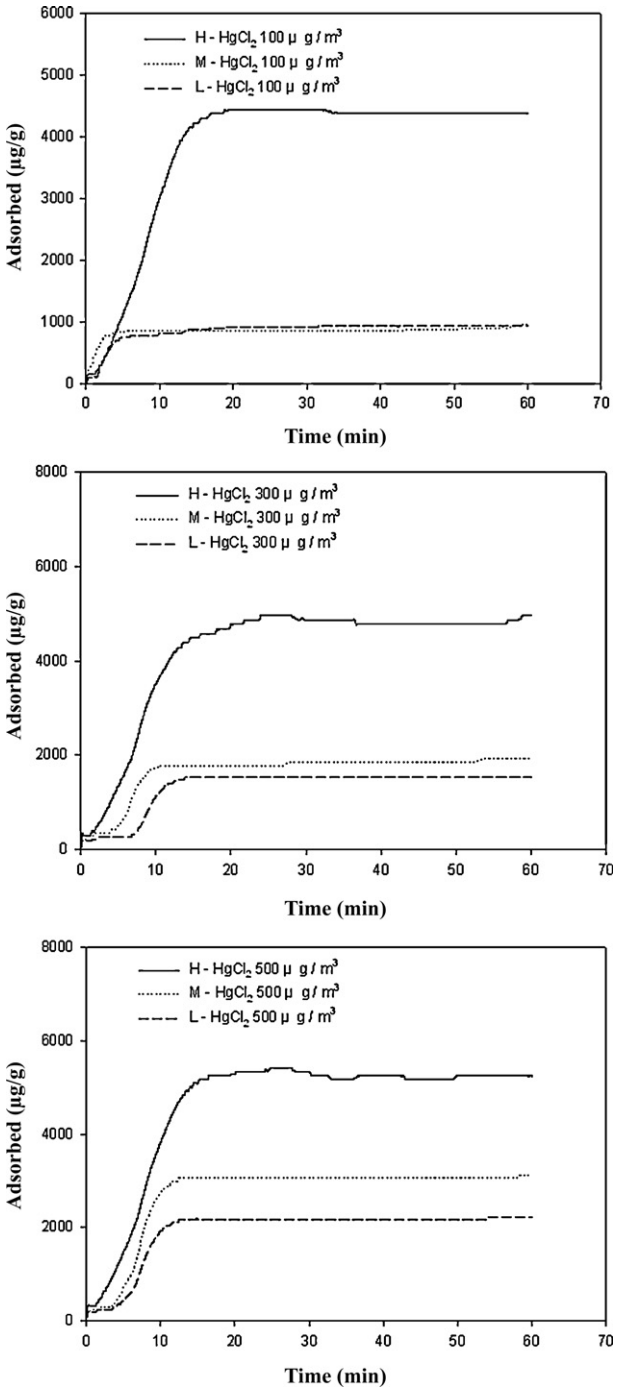

Fig. 5. The adsorption of $HgCl_2$ by the Na_2S+S^0 sulfur-impregnated AC for influent $HgCl_2$ concentration of (a) 100 μg/m³, (b) 300 μg/m³, and (c) 500 μg/m³ (adsorption temperature: 150 °C).

AC. Fig. 6 illustrates that at the adsorption temperatures of 150, 200, and 300 °C, the adsorptive capacity of $HgCl_2$ was relatively high. However, at the adsorption temperature of 80 °C, the adsorptive capacity of $HgCl_2$ decreased drastically. The results showed that the adsorption of $HgCl_2$ by the composite sulfur-impregnated AC was dominated by chemisorption and was conductive to high-temperature adsorption. In addition, the physical adsorption of the composite sulfur-impregnated AC at low temperatures did not perform as well as its chemisorption at high temperatures. This is mainly attributed to the fact that the surface of AC's inner pores filled with Na_2S and S^0 after sulfur impregnation, thus physically limiting the adsorptive capacity of $HgCl_2$ at low temperatures. In contrast, when the adsorption temperature increased, the stability of sulfur also rose and the adsorptive capacity of $HgCl_2$ was further enhanced. It is thus concluded that using composite sulfur-impregnated AC is a feasible way to remove $HgCl_2$ at high temperatures due to its high chemically adsorptive capacity of $HgCl_2$.

3.4. Adsorptive capacity of $HgCl_2$ for composite sulfur-impregnated AC produced by different procedures

In this study, two composite sulfur-impregnation procedures were further compared to ascertain their impact on the saturated

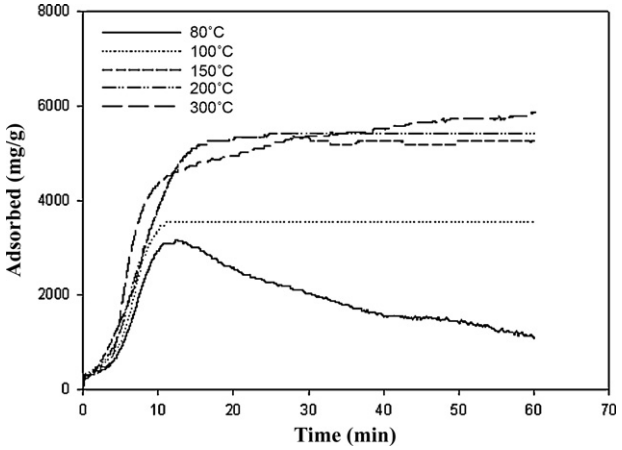

Fig. 6. Variation of $HgCl_2$ adsorptive capacity with adsorption temperatures of 80–300 °C.

adsorptive capacity of $HgCl_2$. The first procedure was conducted to impregnate AC with aqueous-phase Na_2S followed with vapor-phase S^0 (i.e. $Na_2S + S^0$ AC), while the second procedure was conducted in the reverse sequence (i.e. $S^0 + Na_2S$ AC). The $HgCl_2$ adsorption experiments were conducted with the influent $HgCl_2$ concentration of 500 μg/m^3. Fig. 7 shows that, within the adsorption time of 60 min, the adsorptive capacity of $HgCl_2$ for $Na_2S + S^0$ AC reached up to 5236 μg/m^3, while that of $S^0 + Na_2S$ AC was only 2324 μg/m^3. The adsorptive capacity of $HgCl_2$ for the former procedure was approximately 2.25 times higher than that of the latter procedure. The difference in the adsorptive capacity of $HgCl_2$ was attributed to the fact that sulfur can mostly penetrate to the inner pores of sulfurized AC produced by the sequence of aqueous-phase Na_2S and the vapor-phase S^0 impregnation. However, in the sequence of vapor-phase S^0 and aqueous-phase Na_2S impregnation, most micropores could be plugged by Na_2S. Previous research reported that impregnation of S^0 at 400 °C or higher could effectively open the plugged micropores of sulfurized AC, and thus increase the specific surface area of AC and its adsorptive capacity of $HgCl_2$ [14].

3.5. Comparison of $HgCl_2$ adsorptive capacity between composite and single sulfur-impregnated ACs

The saturated adsorptive capacity of $HgCl_2$ for the composite sulfurized AC ($Na_2S + S^0$ AC) was further compared to those for the single sulfurized AC (Na_2S or S^0 AC) at the adsorption temperature

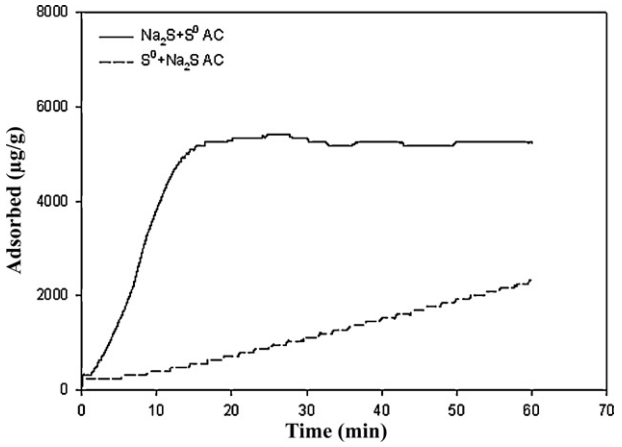

Fig. 7. The influence of composite sulfur-impregnation procedures ($Na_2S + S^0$ AC and $S^0 + Na_2S$ AC) on the adsorptive capacity of $HgCl_2$ (adsorption temperature: 150 °C).

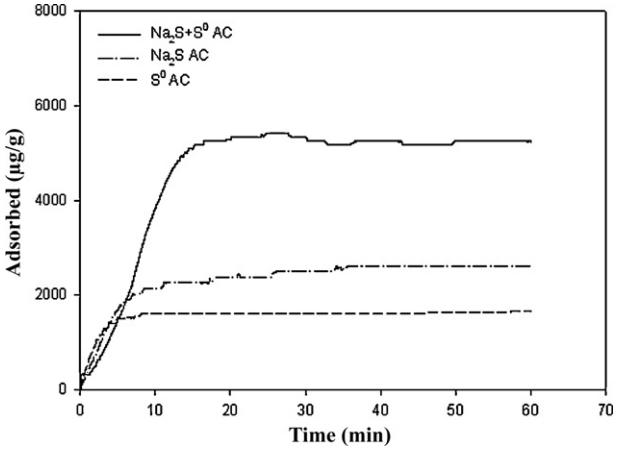

Fig. 8. Comparison of composite sulfur-impregnated AC ($Na_2S + S^0$ AC) with single sulfur-impregnated AC (Na_2S or S^0 AC) at the influent $HgCl_2$ concentration of 500 μg/m^3 (adsorption temperature: 150 °C).

of 150 °C and the influent $HgCl_2$ concentration of 500 μg/m^3. Previous study showed that a maximum saturated adsorptive capacity of 72 μg-$HgCl_2$/g-C was reached for the Na_2S AC [28], which was far below the saturated adsorptive capacity of $HgCl_2$ for the composite sulfurized AC obtained from this study. The results indicated that the adsorption of $HgCl_2$ at high temperatures can be effectively enhanced by impregnating AC with $Na_2S + S^0$. To further prove that the saturated adsorptive capacity of $HgCl_2$ for the composite sulfurized AC was much higher then those for the single sulfurized AC, $HgCl_2$ adsorption experiments were conducted. As illustrated in Fig. 8, the corresponding adsorptive capacity of $HgCl_2$ for the composite sulfurized AC ($Na_2S + S^0$), the Na_2S impregnated AC, and the S^0 impregnated AC were 5236, 2623, and 1653 μg-$HgCl_2$/g-C, respectively. The saturated adsorptive capacity of $HgCl_2$ for the composite sulfurized AC ($Na_2S + S^0$) was nearly the sum of those for two single sulfurized ACs (Na_2S or S^0). The results indicated that the impregnation of Na_2S and S on AC could effectively enhance the adsorption of $HgCl_2$.

4. Conclusions

The innovative composite sulfur-impregnation process successfully combined the impregnation of vapor-phase S^0 and aqueous-phase Na_2S onto the surface of activated carbons originally derived from the pyrolysis of waste tires. The adsorptive capacity of $HgCl_2$ increased with the sulfur content and specific surface area of composite sulfur-impregnated AC, the influent $HgCl_2$ concentration, and the adsorption temperature. A maximum adsorptive capacity of $HgCl_2$ up to 5236 μg-$HgCl_2$/g-C was observed for the composite $Na_2S + S^0$ AC, which was approximately 2.00 and 3.17 times higher than those for the single Na_2S and S^0 ACs, respectively. Further investigation on the sequence of the composite sulfur-impregnated procedure indicated that the adsorptive capacity of $HgCl_2$ for AC impregnated with aqueous-phase Na_2S and followed by vapor-phase S^0 was approximately 2.25 times higher than that for AC impregnated with vapor-phase S^0 and followed by aqueous-phase Na_2S. Among the various conditions studied, the impregnation of S^0 at 400 °C or higher could effectively open the plugged micropores of sulfurized AC, and thus increased the specific surface area of AC and its adsorptive capacity of $HgCl_2$. Furthermore, the adsorptive capacity of $HgCl_2$ at temperatures below 70 °C was dominated by physical adsorption, while that above 70 °C was dominated by chemisorption.

Acknowledgments

This study was performed under the auspices of National Science Council, Republic of China, under contract number NSC 98-2221-E-016-MY3. The authors are grateful to National Science Council for its financial support.

References

[1] S.X. Wang, L. Zhang, G.H. Li, Y. Wu, J.M. Hao, N. Pirrone, F. Sprovieri, M.P. Ancora, Mercury emission and speciation of coal-fired power plants in China, Atmos. Chem. Phys. 10 (2010) 1183–1192.
[2] T.A. Brady, M. Rostam-Abadi, M.J. Rood, Applications for activated carbons from waste tires: natural gas storage and air pollution control, Gas Sep. Purif. 10 (1996) 97–102.
[3] J.L. Allen, J.L. Gatz, P.C. Eklund, Application for activated carbons from used tires: butane working capacity, Carbon 37 (1999) 1485–1489.
[4] Y.R. Lin, H. Teng, Mesoporous carbons from waste tires char and their application in wastewater discoloration, Microporous Mesoporous Mater. 54 (2002) 167–174.
[5] C.S. Yuan, H.Y. Lin, C.H. Wu, M.H. Liu, Preparing of sulfurized powdered activated carbon from waste tires using an innovative compositive impregnation process, J. Air Waste Manage. Assoc. 54 (2004) 862–870.
[6] H.Y. Lin, C.S. Yuan, C.H. Wu, C.H. Hung, The adsorptive capacity of vapor-phase mercury chloride onto powdered activated carbon derived from waste tires, J. Air Waste Manage. Assoc. 56 (2006) 1558–1566.
[7] P.T. Williams, S. Besleri, Pyrolysis–thermogravimetric analysis of tyre components, Fuel 74 (1995) 1277–1283.
[8] H.Y. Lin, C.S. Yuan, W.C. Chen, Determination of adsorptive capacity and adsorption isotherm of gas-phase mercury chloride on powdered activated carbon using thermogravimetric analysis, J. Air Waste Manage. Assoc. 56 (2006) 1550–1557.
[9] F.S. Cannon, J.S. Dusenbury, J. Paulsen, D.W. Sigh, D.J. Maurer, Advanced oxidant regeneration of granular activated carbon for controlling air-phase VOCs, Ozone Sci. Eng. 18 (5) (1996) 417–441.
[10] M. Popescu, J.P. Jolu, J. Carre, C. Danatoiu, Dynamic adsorption and temperature programmed desorption of VOCs on activated carbons, Carbon 41 (2000) 739–748.
[11] M. Fan, R.C. Brown, Comparison of the loss-on-ignition and thermogravimetric analysis techniques in measuring unburned carbon in coal fly ash, Energy Fuel 15 (2001) 1414–1417.
[12] Y. Xiong, T. Jiang, X. Zou, Automatic proximate analyzer of coal based on isothermal thermogravimetric analysis (TGA) with twin-furnace, Thermochim. Acta 408 (2003) 97–101.
[13] R.D. Vidic, M.T. Chang, R.C. Thurnau, Kinetics of vapor-phase mercury uptake by virgin and sulfur-impregnated activated carbon, J. Air Waste Manage. Assoc. 48 (1998) 247–255.
[14] L. Wei, R.D. Vidic, T.D. Brown, Optimization of sulfur impregnation protocol for fixed-bed application of activated carbon-based sorbents for gas-phase mercury removal, ES&T 32 (1998) 531–538.
[15] W.C. Chen, H.Y. Lin, C.S. Yuan, C.H. Hung, Kinetic modeling on the adsorption of mercury chloride vapor on spherical activated carbon by thermogravimetric analysis, J. Air Waste Manage. Assoc. 59 (2009) 227–235.
[16] F. Wenguo, B. Eric, D.V. Radisav, Sulfurization of carbon surface for vapor phase mercury removal. I: Effect of temperature and sulfurization protocol, Carbon 44 (2006) 2990–2997.
[17] J.W. Graydon, X. Zhang, D.W. Kirk, C.Q. Jia, Sorption and stability of mercury on activated carbon for emission control, J. Hazard. Mater. 168 (2009) 978–982.
[18] A. Gomez-Serrano, A. Macias-Garcia, A. Espinosa-Mansilla, C. Valenzulela-Calahorro, Adsorption of mercury, cadmium and lead from aqueous-solution on heat-treated and sulphurized activated carbon, Water Res. 32 (1998) 1–4.
[19] T. Morimoto, S. Wu, M.A. Uddin, Characteristics of the mercury vapor removal from coal combustion flue gas by activated carbon using H_2S, Fuel 84 (2005) 1968–1974.
[20] J.A. Korpiel, R.D. Vidic, Effect of sulfur impregnation method on activated carbon uptake of gas-phase mercury, ES&T 31 (1997) 2319–2325.
[21] W.C. Chen, C.S. Yuan, C.H. Hung, H.Y. Lin, Sorption phenomenon of mercury chloride from saturated powdered activated carbons by using thermogravimetric analysis, J. Environ. Eng. Manage. 19 (4) (2009) 213–220.
[22] T.C. Ho, P. Yang, T.H. Kuo, J.R. Hopper, Characteristics of mercury desorption from sorbents at elevated temperatures, Waste Manage. 18 (1998) 445–452.
[23] F. Rodriguez-Reinoso, The role of carbon materials in heterogeneous catalysis, Carbon 36 (1998) 159–175.
[24] V. Sandra, P. Roberto, Desorption of sulfur from H_2S on porous adsorbents and effect on their mercury adsorption capacity, Geothermics 28 (1999) 341–354.
[25] S. Wu, M.A. Uddin, E. Sasaoka, Characteristics of the removal of mercury vapor in coal derived flue gas over iron oxide sorbents, Fuel 85 (2006) 213–218.
[26] H.C. Hsi, M.J. Rood, M. Rostam-Abadi, S. Chen, R. Chang, Effects of sulfur impregnation temperature on the properties and mercury adsorption capacities of activated carbon fibers, Environ. Sci. Technol. 35 (2001) 2785–2791.
[27] S.H. Lee, Y.O. Park, Gas-phase mercury removal by carbon-based sorbents, Fuel Process. Technol. 84 (2003) 197–206.
[28] H.Y. Lin, W.C. Chen, C.S. Yuan, C.H. Hung, Surface functional characteristics (C, O, S) of carbon black before and after steam activation, J. Air Waste Manage. Assoc. 58 (2008) 78–84.